

Measuring primordial gravitational waves from CMB B -modes in cosmologies with generalized expansion histories

Claudia Antolini,^{*a,b*} Matteo Martinelli,^{*a,b*} Yabebal Fantaye,^{*a,b*} Carlo Baccigalupi^{*a,b*}

^{*a*}SISSA, Via Bonomea 265, Trieste, I-34136, Italy

^{*b*}INFN, Sezione di Trieste, Via Valerio 2, 34127 Trieste, Italy

E-mail: claudia.antolini@sissa.it, mmartin@sissa.it, fantaye@sissa.it, bacci@sissa.it

Abstract. We evaluate our capability to constrain the abundance of primordial tensor perturbations (primordial gravitational waves, PGWs) in cosmologies with generalized expansion histories in the epoch of cosmic acceleration. Forthcoming satellite and sub-orbital experiments probing polarization in the Cosmic Microwave Background (CMB) are expected to measure the B -mode power in CMB polarization, coming from PGWs on the degree scale, as well as gravitational lensing on arcminute scales; the latter is the main competitor for the measurement of PGWs, and is directly affected by the underlying expansion history, determined by the presence of a Dark Energy (DE) component. In particular, we consider early DE possible scenarios, in which the expansion history is substantially modified at the epoch in which the CMB lensing is most relevant. We show that the introduction of a parametrized DE may induce a variation as large as 30% in the ratio of the power of lensing and PGWs on the degree scale. We find that adopting the nominal specifications of upcoming satellite measurements, the constraining power on PGWs is weakened by the inclusion of the extra degrees of freedom, resulting in a reduction of about 10% of the upper limits on r in fiducial models with no GWs, as well as a comparable increase in the error bars in models with non-zero tensor power. Moreover, we find that the inclusion of sub-orbital CMB experiments, capable of mapping the B -mode power up to the angular scales which are affected by lensing, has the effect of restoring the forecasted performances with a fixed cosmological expansion history corresponding to a cosmological constant. Finally, we show how the combination of CMB data with Type Ia SuperNovae (SNe), Baryonic Acoustic Oscillations (BAO) and Hubble constant allows to constrain simultaneously the primordial tensor power and the DE quantities in the parametrization we consider, consisting of present abundance and first redshift derivative of the energy density. We compare this study with results obtained using the forecasted lensing potential measurement precision from CMB satellite observations, finding consistent results.

Keywords: gravitational waves and CMBR polarization, weak gravitational lensing

ArXiv ePrint: [1208.3960](https://arxiv.org/abs/1208.3960)

Contents

1	Introduction	1
2	Generalized expansion histories: how lensing affects the CMB spectra	2
3	Simulated data and analysis	5
4	Results	9
5	Concluding remarks	11

1 Introduction

Anisotropies in the Cosmic Microwave Background (CMB) represent one of the pillars of modern cosmology. Their statistical distribution, characterized primarily by the angular power spectrum, is consistent with a flat Friedmann Robertson Walker metric, expanding at a Hubble rate corresponding to about 70 km/s/Mpc, and composed by three main cosmological components, namely baryons and leptons representing about 4% of the total energy density, dark matter (DM, about 21%) constituting the large part of the gravitational potential around collapsed or forming cosmological structures, and about 75% of a Dark Energy (DE) component, similar or coincident with a Cosmological Constant (CC), responsible for a late time phase of accelerated expansion. The primordial spectrum of density perturbations is almost scale invariant, corresponding to a Harrison-Zel'dovich power law shape in wavenumbers. Three satellites have been observing CMB anisotropies, the Cosmic Background Explorer [1], the Wilkinson Microwave Anisotropy Probe [2], and Planck, which is expected to release cosmological data in early 2013 [3]. Space observations will provide an all sky measurement of total intensity and polarization anisotropies down to a resolution of a few arcminutes, and a sensitivity of a few μK per resolution element.

A number of sub-orbital experiments are planned and have been observing selected regions of the sky and frequency spectrum, looking for arcminute and sub-arcminute scale anisotropies in total intensity (T), as well as polarization¹. These observations will target most important and yet still undetected effects, dominating the curl component (B -modes) of the linear polarization pattern in CMB anisotropies [4, 5]. On arcminute angular scales, the latter are dominated by the gravitational lensing of the anisotropies at last scattering by means of forming cosmological structures along the line of sight. A fraction of the gradient component of polarization (E -modes), dominating because powered by density fluctuations responsible for sub-degree acoustic oscillations at last scattering, is converted into B -modes by means of gravitational lensing [6]. The power spectrum of the underlying DM distribution, and the primordial E -modes, produce a characteristic and broad lensing peak centered at $l \simeq 1000$ in the B -mode power spectrum. Gravitational lensing has been recently detected in the damping tail of T anisotropies by several groups [7, 8], also cross-correlating the lensing with observed structures [9], while B -modes have not yet been detected, see The Quiet Collaboration [10] for the current upper limits. On the degree angular scales on the other hand, a primordial spectrum of tensor anisotropies or cosmological Gravitational Waves

¹see NASA ADS for the list of operating or planned sub-orbital CMB experiments.

(GWs) would produce a narrow peak, rapidly vanishing on sub-degree angular scales, not supported by radiation pressure from massive particles, as is instead the case for T and E -modes. On large angular scales, corresponding to several degrees in the sky, the decay of the GWs tail in the B -modes can be re-amplified through re-scattering onto electrons in the epoch of cosmic reionization. As for the case of lensing, only upper limits exist for the amplitude of PGWs through direct measurement of B -modes. The two effects compete for detection, and their different origin, primordial and linear for GWs, late and second order for lensing, has been exploited for designing separation techniques [12]. Furthermore, it has been analysed in the past how an accelerated expansion modifies the shape of the spectrum of PGWs as a result of propagation in a different space-time [11].

The lensing peak of B -mode anisotropies strongly depends on the history of cosmic expansion. It has been shown [13] that its amplitude may undergo variations of order 10% if the DE is dynamical at the epoch corresponding to the onset of acceleration, i.e. about $z \simeq 1$, in which its actual amplitude is poorly constrained by existing measurements of the CMB or large scale structures. The B -mode lensing peak as a DE probe has been investigated by several authors [13, 14], who in particular have shown how the lensing is capable of breaking the projection degeneracy affecting CMB anisotropies at the linear level, as it was recently confirmed in the context of lensing detection for sub-orbital T -mode experiments [15]. On the other hand, the detection thresholds for cosmological GWs as well as the accuracy on DE constraints from CMB observations have never been given by taking into account the full set of degrees of freedom, represented not only by the amplitude of primordial GWs, but also by those related to the expansion history, parametrized through suitable DE models. The release of the latter degrees of freedom in the context of experiments aiming at the detection and characterization of B -mode anisotropies is expected to have a direct impact in the quoted detection thresholds of primordial GWs.

In this work we explore this issue, by investigating the sensitivity of forthcoming B -mode probes on primordial GWs abundance as well as DE dynamics when all the physical degrees of freedom shaping the B -mode power spectrum are considered and treated jointly. In this context, we consider in particular the interplay between satellite measurements, accessing large scale polarization and extracting lensing mainly from T and E measurements, and the case of sub-orbital ones, directly probing lensing B -modes. We will take as reference two among the most important forthcoming B -mode probes, EBEX [16] and PolarBear [17] as well as the all sky measurements featuring the nominal capabilities from Planck [18].

This work is organized as follows. In Section 2 we describe the impact of a modified expansion history on the CMB lensing power. In Section 3 we describe our set of simulated data as well as the reference experiments we consider. In Section 4 we show and discuss our results, while in Section 5 we draw our conclusions.

2 Generalized expansion histories: how lensing affects the CMB spectra

In this work we consider models of expansion history corresponding to a Cosmological Constant (CC) and its generalization through the equation of state $w = p/\rho$ of the DE evaluated at present, as well as its first derivative in the scale factor [19, 20], often labelled CPL. In this modelisation, the DE equation of state and the ratio Ω_{DE} of its energy density with respect to the cosmological critical density are given by

$$p = [w_0 + (1 - a)w_a] \rho \quad , \quad \Omega_{DE}(z) = \Omega_{DE,0} e^{3 \int_0^z dz' \frac{1+w(z')}{1+z'}} \quad . \quad (2.1)$$

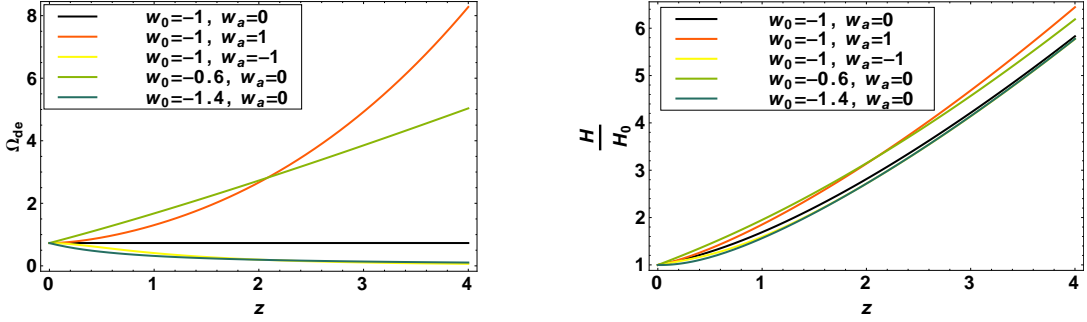


Figure 1. Left panel: redshift evolution of the DE component with different values of w_0, w_a . As the sum w_0, w_a get above -1 , the DE term becomes increasingly important in the past. Right panel: corresponding evolution of the Hubble parameter with redshift with the same expansion histories considered in the left panel.

Such a parametrization allows for a large set of dynamics in the cosmic acceleration, and in particular an increased DE abundance at the equivalence with cold DM and the onset of acceleration. In the following we will see how the evolution of DE with time affects the CMB lensing because of its influence on the structures generating the gravitational potential responsible for the deflection. In Fig. 1, left panel, one can see how the DE density evolves with time as the w_0, w_a parameters vary. In order to get a glimpse on how the lensing process is modified by different expansion histories, let's look again at Eq. (2.1) and consider how this influences the evolution with redshift of the Hubble parameter $H(z)$, which we can see in Fig. 1 (right panel).

Gravitational lensing deflection angle is related to the lensing projected potential ϕ (see e.g. [24, 25]) through the relation

$$d_l^m = -i\sqrt{l(l+1)}\phi_l^m. \quad (2.2)$$

It is characterized by the lensing deflection power spectrum C_ℓ^{dd} , which is defined through the ensemble average

$$\langle d(a, b)_L^{M*} d(a', b')_{L'}^{M'} \rangle \equiv \delta_L^{L'} \delta_M^{M'} (C_L^{dd} + N_L^{aa'bb'}). \quad (2.3)$$

Following [26], the lensing deflection angle can be inferred by the observed CMB anisotropies through

$$d(a, b)_L^M = n_L^{ab} \sum_{l'l''} W(a, b)_{ll''}^{mm'M} a_l^m b_{l''}^{m'}, \quad (2.4)$$

where a, b are the CMB modes T, E, B modes, n_L^{ab} is a normalization factor introduced to obtain an unbiased estimator and $W(a, b)$ is a weighting factor which leads to the noise $N_L^{aa'bb'}$ on the power spectrum².

We now describe from a physical point of view the CMB lensing process and its sensitivity to the underlying expansion history. For a full mathematical treatment we refer to earlier works [21–23]. As the Hubble expansion rate grows in the past with respect to Λ CDM, the cosmic expansion rate increases. Its value at the epoch of structure formation will determine how efficient the process of structure formation is, and consequently the abundance of available

²We will specify the extraction method followed here (and therefore our choice of W) in the next section.

lenses: the lower is the Hubble rate in that epoch, the lower the friction represented by the expansion with respect to structure formation, the higher the number of lenses will be. As noticed by Acquaviva & Baccigalupi [13], the latter occurrence is rather sensitive to the DE abundance at the epoch at which lensing is most effective, $z \simeq 1 \pm 0.5$, and rather independent of the DE properties at earlier and later epochs than that, simply because by geometry, the lensing cross section peaks about halfway between sources and observer. The distribution

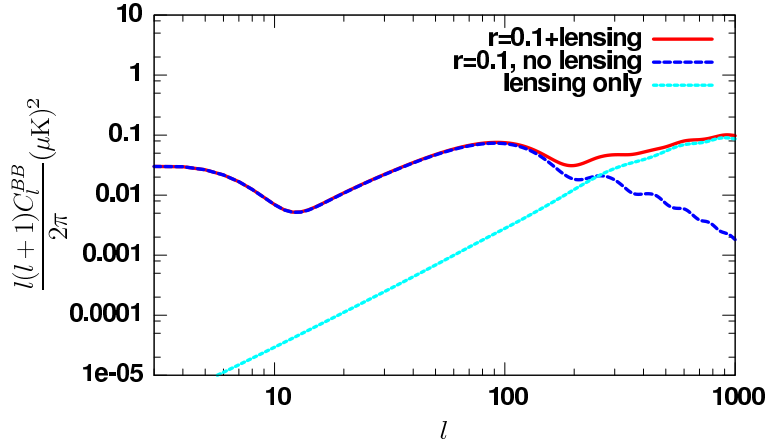


Figure 2. B -modes for CMB polarization anisotropies with different contributions given by primordial tensor modes only with $r = 0.1$ (green), by lensing only (blue), and the total for both lensing and $r = 0.1$ tensor modes.

of lenses, following the power spectrum of density perturbations, as well as the geometrical properties mentioned above, determine the efficiency of CMB lensing to peak on arcminute angular scales, corresponding to structures from a few to about 10^2 comoving Mpc. Being a non-linear effect, lensing redistributes primordial anisotropy power of single multipoles at last scattering on a finite interval of scales. The net effect on T and E is a smearing of acoustic peaks and the dominance in the damping tail region, corresponding to multipoles of $\ell \gtrsim 1000$, where primordial anisotropies die out because of diffusion damping, and the only power comes from larger scales because of lensing. As we already discussed, for B -modes the effect is rather different. In Fig. 2 we show the various contributions to B -modes, coming from primordial GWs on degree and super-degree angular scales, and from lensing on arcminute ones. The latter effect arises because a fraction of E -modes is transferred to B because of the deflection itself. The sensitivity of this process to the underlying DE properties is described in Fig. 3, where the T and B spectra are shown for various cases. The geometric shift in T is due to the change in comoving distance to the last scattering, given by

$$d_{LS} = H_0^{-1} \int_0^{z_{LS}} dz \left[\Omega_m (1+z)^3 + \Omega_{DE,0} e^{3 \int_0^z dz' \frac{1+w(z')}{1+z'}} \right]^{-1/2} \quad (2.5)$$

where H_0 is the Hubble parameter, Ω_m is the matter abundance today relative to the critical density and the contributions from radiation and curvature are neglected. Clearly, the same value of d_{LS} can be obtained with various combinations of parameters, including the DE, creating the so called projection degeneracy, already addressed in [13]. The lensing, for B -modes in particular, shown in the right panel, is capable of breaking it, because of its sensitivity to the DE abundance at the epoch in which its cross section is non-zero. Indeed,

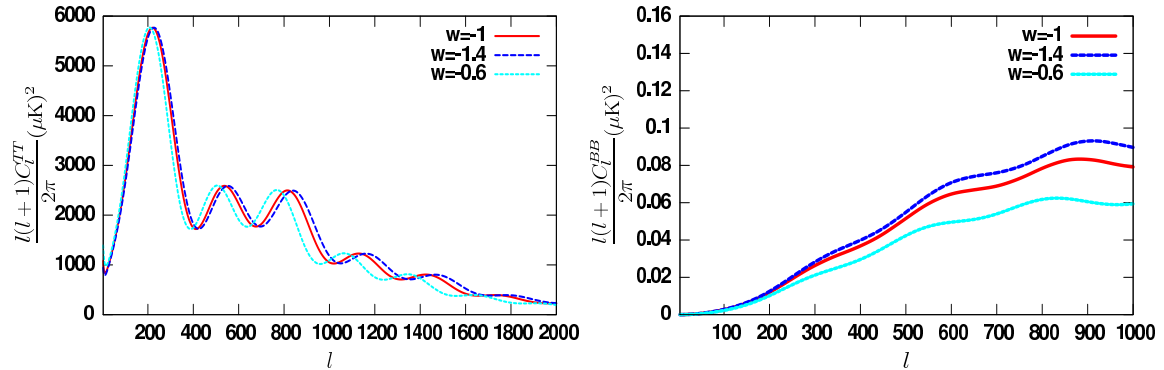


Figure 3. Left panel: Variation of the T -mode spectrum with different values of w . Right panel: Variation of the B -mode spectrum with different values of w .

looking again at Fig. 1, we see that the DE density at the epoch we are considering follows an opposite behaviour with respect to the curves represented in Fig. 3: the lower the curve, the higher the value of the expansion rate at the relevant epoch for lensing leading to an increasing suppression of the power, the higher the dark energy density, as already discussed above. It is already well known [27] that the gravitational lensing signal constitutes a fundamental contaminant in the PGWs spectrum. The latter is parametrized by the ratio between the tensor and scalar power in the primordial perturbation power spectra, r . As for scalars, the power spectrum of PGWs is also characterized by a spectral index. We work here in the hypothesis of single field inflationary models, which relate the tensor spectral index to r , without introducing any additional parameter; a discussion on parameter estimation without this assumption may be found in [28, 29].

Our aim in this work is trying to infer how a simultaneous constraint can be affected by the presence of both signals in data, and in particular to determine the degradation, if any, of the constraint on r as the background expansion is allowed to vary according to a CPL parametrization. As we have seen, this heavily affects the lensing peak of the CMB: for a better quantification of this point, we show in Fig. 4 how the ratio of the two contributions at the peak of the GWs power, corresponding to $\ell \simeq 100$, can vary macroscopically because of the variation in the DE dynamics, reaching 50%. It is clear that it is necessary to study the parameter space represented by r , w_0 , w_a jointly, in order to understand the constraining power based on data on CMB B -modes.

3 Simulated data and analysis

In this Section we describe our methodology related to the simulation of CMB data as well as its analysis. In order to obtain a forecast for different parameters using nominal instrumental performances, a Fisher matrix approach is often adopted for estimating covariances. However, the latter approach is rigorously valid only if the likelihood shape of parameters is Gaussian. In our case, as we will show, the shape of the likelihood for r deviates substantially from a Gaussian; in order to avoid inaccuracies, as it was pointed out in recent works [30] we prefer to avoid such a simplification. Another reason for doing so is that we will make use of different datasets in our analysis, described later in this Section, and we cannot assume that no degeneracies will arise from this combination. For these reasons, our approach consists

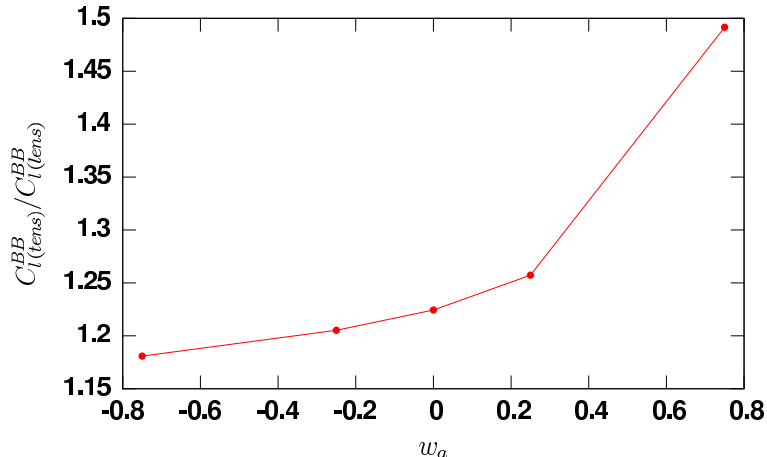


Figure 4. Ratio between the primordial B -modes ($r = 0.05$) and lensing generated B -modes at $\ell = 100$ with different expansion histories with w_0 fixed to -1.

in computing the full likelihood shapes by using a Markov chains approach. We exploited extensively the publicly available software package `cosmomc`³ for Markov Chain Monte Carlo (MCMC) analysis of CMB datasets [31].

We create simulated CMB datasets for T , E and B -modes, adopting the specifications of Planck [3], EBEX [16] and PolarBear [32] experiments. In Table 2 we list the relevant parameters adopted in the present work. The fiducial model for the standard cosmological parameters is the best fit from the WMAP seven years analysis [2], concerning flat Λ CDM parametrizing the abundances of CDM and baryons plus leptons ($h^2\Omega_c$, $h^2\Omega_b$, respectively), $100 \cdot \theta$, where θ is the ratio of the sound horizon to the angular diameter distance, the optical depth τ of cosmological reionization, the spectral index n_s and amplitude A_s of the primordial power spectrum of density perturbations, the parameters for evolving DE w_0 , w_a . In the present work we want to study the effects that a generalized expansion history has on the cases of a null as well as a positive detection of r . In Table 1 the values used to compute the simulated spectra are shown.

$h^2\Omega_b$	$h^2\Omega_c$	$100 \cdot \theta$	τ	n_s	A_s	w_0	w_a
0.02258	0.1109	1.0388	0.087	0.963	$2.43 \cdot 10^{-9}$	-1	0

Table 1. Set of cosmological parameters and adopted values for the cases $r = 0$ and $r = 0.05$ of simulated data.

Therefore, two different fiducial models were adopted concerning the amplitude of primordial GWs, corresponding to their absence ($r = 0$) and to $r = 0.05$. The latter case corresponds to a detectable value also in a more realistic case in which data analysis includes foreground cleaning and power spectrum estimation is chained to the MCMCs [33, 34].

Using these sets we compute the fiducial power spectra C_ℓ^i with $i = TT, TE, EE, BB$, in order to compare them with the theoretical models generated by exploring the parameter space. In this work we make use of the `cosmomc` package for that. We add a noise bias to these fidu-

³cosmologist.info

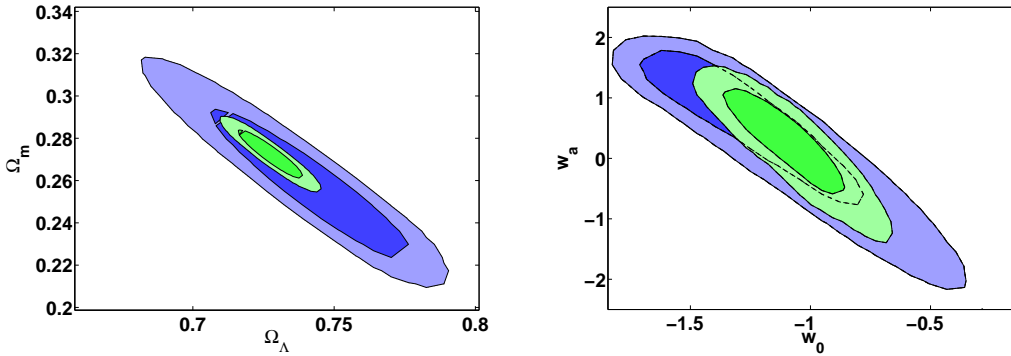


Figure 5. Test analysis with $r = 0$, evolving DE. Left panel: 1 and 2σ contours $\Omega_m - \Omega_\Lambda$ diagram. In blue the combination PolarBear + Planck with dynamical DE, in green PolarBear + Planck, with Λ CDM. Right panel: 1 and 2σ contours for $w_a - w_0$. In blue the results obtained when SNe are not included, in green when SNe data were considered.

cial spectra, consistently with the mentioned instrumental specifications. For each frequency channel which is listed in Table 2, the detector noise considered is $w^{-1} = (\theta\sigma)^2$, where θ is the FWHM (Full-Width at Half-Maximum) of the instrumental beam if one assumes a Gaussian and circular profile and σ is the sensitivity ΔT . To each of the C_ℓ coefficients the added contribution from the noise is given by: $N_\ell = w^{-1}e^{(\ell(\ell+1)/\ell_b^2)}$, where ℓ_b is given by $\ell_b \equiv \sqrt{8\ln 2}/\theta$. The MCMCs were conducted by adopting a convergence diagnostic based on the Gelman and Rubin statistics [35]. We sample eight cosmological parameters ($\Omega_b h^2$, $\Omega_c h^2$, τ , n_s , A_s , Ω_Λ , z_{reion} , as well as the Hubble expansion rate H_0), the w_0 and w_a DE parameters, and r adopting flat priors. We make use of priors coming from different probes in the `cosmomc` package, specifically Baryon Acoustic Oscillations (BAO) [36, 37], Supernovae (SNe) data [38], results from the Hubble Space Telescope (HST) [39].

In order to calibrate our pipeline, we first consider a Λ CDM model with $r = 0$, varying both the DE parameters w_0 , w_a or keeping them fixed to a CC through the MCMCs, and considering for simplicity the combination of Planck and one sub-orbital experiment (PolarBear). The results in the $(\Omega_\Lambda, \Omega_m)$ plane are shown in Fig. 5 (left panel), showing the 1 and 2σ contours for the case of a Cosmological Constant (green) and dynamical DE (blue). The decrease in constraining power due to the extra degrees of freedom is evident, although the shape of the contour regions is rather stable. Our interpretation is that the introduction of new degrees of freedom affects the precision on the measurement of the two parameters considered. On the other hand, the distance to last scattering is degenerate between cosmological abundances and expansion history, resulting in a geometric degeneracy for the non-lensed pure CMB dataset. Our forecasted datasets contain both CMB lensing measurements, as well as external data on the recent expansion history; we see here how this procedure eliminates such degeneracies. The residual effect is represented by a loss of precision due to the higher dimension of the parameter space, accounting now for a dynamical DE. We further investigate this point in the right panel of Fig. 5, where the results in presence (green) or absence (blue) of the SNe measurements are shown, confirming the substantial relevance of external measurements of the expansion history at low redshift, as anticipated in earlier works [14].

It is interesting to compare the present case in which lensing B -modes are probed directly by CMB sub-orbital experiments with the case in which the lensing is extracted from

Experiment	Channel	FWHM	$\Delta T/T$
Planck	70	14'	4.7
	100	9.5'	2.5
	143	7.1'	2.2
	217	5.0'	4.8
$f_{sky} = 0.85$			
EBEX	150	8'	0.33
	250	8'	0.33
	410	8'	0.33
$f_{sky} = 0.01$			
PolarBear	90	6.7'	0.41
	150	4.0'	0.62
	220	2.7'	2.93
$f_{sky} = 0.03$			
CMBpol	70	12'	0.148
	100	8.4'	0.151
	150	5.6'	0.177
$f_{sky} = 0.85$			

Table 2. Planck, EBEX, PolarBear and CMBpol performance specifications. Channel frequency is given in GHz, beam FWHM in arcminutes, and the sensitivity for T per pixel in $\mu\text{K}/\text{K}$. The polarization sensitivity for both E and B -modes is $\sqrt{2}\Delta T/T$.

all sky CMB anisotropy maps as expected by adopting the nominal performance of operating (Planck) and proposed post-Planck polarisation dedicated CMB satellites (see CMBpol and the COsmic Origin Explorer (CORE) [40, 41]); the latter cases will give us an estimate of the improvement in the constraining power on w_0, w_a as a function of the satellite instrumental specifications. A similar approach has already been applied to the TT spectrum by the SPT collaboration in [42]; the case for this analysis is different since the focus is set on the B -modes. We create simulated datasets for Planck and CMBpol, adopting nominal performances as in the previous case, but adding the forecasted lensing potential measurements. Our aim is to quantify, in these cases, the efficiency on determination of the expansion parameters w_0 and w_a , and how they scale with satellite instrumental capabilities, reaching cosmic variance limit also for polarization as in the cases of planned post-Planck satellite CMB experiments; therefore we keep $r = 0$ fixed and let the CPL parameters vary. We use the lensing extraction method presented in [26] where the authors construct the weighting factor W of Eq. (2.4) as a function of CMB power spectra C_{ab} , with $ab = TT, TE, EE, EB, TB$. The BB spectrum is excluded because the adopted method is only valid when the lensing contribution is negligible compared to the primary anisotropies; this assumption fails for B -modes, which are not considered in this analysis, by modifying `cosmomc` according with [24]. This aspect, as well as the instrumental sensitivity, implies that lensing measurements in this case come mainly from sub-degree T and E anisotropy data. We study the constraining power on CPL parameters from Planck data in three cases: first, when lensing measurements are used, second, without lensing, but with the inclusion of the priors introduced above (BAO, HST, SNe), and finally using both. We performed this analysis also on a CMBpol-like experiment using the specifications in [40]; the major uncertainty on the data from such an experiment

will be due to cosmic variance. Results are presented in Table 3.

Let us focus first on the comparison between CMB satellite lensing measurements and the

Planck	CMB+lensing extraction	CMB+priors	CMB+lensing extraction+priors
$\Delta(w_0)$	0.5	0.2	0.2
$\Delta(w_a)$	1.1	0.6	0.6
CMBpol	CMB+lensing extraction	CMB+priors	CMB+lensing extraction+priors
$\Delta(w_0)$	0.4	0.159	0.150
$\Delta(w_a)$	1.0	0.57	0.497

Table 3. 1σ uncertainties on CPL parameters w_0 , w_a for Planck and for a CMBpol specifications when using lensing extraction, when using external priors and when combining both, in the case $r = 0$.

case in which the lensing is probed through the lensing dominated part of the B -mode spectrum. As it can be seen comparing with the contours in Figure 5, the relevance of lensing measurements is comparable in the two cases; moreover, it is found that the priors have a comparable relevance. We conclude that satellite lensing measurements using T and E , and sub-orbital ones directly accessing lensing B -modes, have a comparable capability for constraining the expansion history. Both cases are relevant to study, as the impact of non-idealizations including systematics as well as removal of foreground emissions may produce different outcomes [43, 44]. Let us now discuss the differences between the case of Planck, which is a cosmic variance limited experiment for total intensity, with respect to the enhanced capability of planned post-Planck satellites, approaching the same limit for polarization as well. As the results show, the improvement in the instrumental specification does cause an enhancement of the constraining capability corresponding to a factor 20% for w_0 and 10% for w_a ; when priors are considered, the results improve by a factor of about 6% for w_0 and 15% for w_a . We conclude that the improvement is sensible but does not change the order of magnitude of the forecasted precision, and we argue that this is consistent with the fact that Planck is cosmic variance limited in total intensity, which is the dominant part of the CMB anisotropy signal.

In the following we focus on the capability of constraining the expansion parameters using the B -modes, in order to study if new degeneracies arise when the relative amplitude between PGWs (through variations of r) and the lensing spectrum (as traced by lensing B -modes) vary at the same time.

4 Results

We study here the recovery of the primordial tensor to scalar ratio, performed while varying the cosmological expansion history. As we already pointed out, we consider two cases, for a null ($r = 0$) and positive ($r = 0.05$) detection. In both cases, the fiducial DE model is Λ CDM, and the generalized expansion history is parametrized by w_0 and w_a . In order to verify the relevance of sub-orbital probes, probing the lensing peak in the B -mode spectrum, we consider the case of pure satellite CMB data separately from the one with joint satellite and sub-orbital probes.

The results on r as 2σ upper limits and 1σ statistical uncertainties in the null and positive detection cases respectively, as well as the corresponding constrains on CPL parameters

are shown in Table 4. In the case with a non-vanishing fiducial value of r , a change in the MCMC recovered value of r is present when the theoretical model or the experimental configuration are changed. In order to address the reason of the differences in the recovered mean value of r we computed the Gelman and Rubin indicator for the chains we performed, finding that the differences we see can be ascribed to fluctuations in the MCMC procedure (see e.g. [45] for a more specific discussion on this topic). Nevertheless, note that, as expected, the results obtained by adopting the nominal specifications of Planck are in agreement with [46] for Λ CDM. A first result concerns the quantification of precision loss of the recovery on r when a generalized expansion rate is considered, and when only satellite CMB data are considered. This corresponds roughly to 10% for the null and about 5% for positive detections of r . The interpretation is related to the extra degrees of freedom considered, while as in the previous sections, the lensing component of simulated spectra, as well as the priors on the expansion history from external probes, help reducing geometric degeneracies, leaving room only for an increase in the statistical error of the various measurements, which we quantify here. It is interesting now to look at the case when all the CMB probes are considered, verifying that the precision loss in this case falls below a detectable level. This result is uniquely related to the enhanced sensitivity of sub-orbital probes, allowing for a deeper study of the lensed component of CMB spectra, and in particular on the lensing peak in B -modes. Concerning the CPL parameters (w_0, w_a), it is possible to see in Table 4 how the constraints do not degrade switching from the $r = 0$ to the $r = 0.05$ simulated dataset. This shows, as previously stated, that there are no detectable degeneracies between r and CPL parameters in our considered datasets. Moreover we can also notice how constraints on (w_0, w_a) do not improve much if we use sub-orbital experiments alongside satellite data to get better CMB sensitivity; this highlights the fact that the prior we used, most of all the SNe data, are crucial to constrain DE quantities.

Experiments, fiducial	$r = 0$	$r = 0.05$
Planck with priors, Λ CDM	$r < 0.029$	$r = 0.057 \pm 0.022$
Planck with priors, CPL	$r < 0.031$	$r = 0.059 \pm 0.023$
all experiments, Λ CDM	$r < 0.025$	$r = 0.057 \pm 0.020$
all experiments, CPL	$r < 0.025$	$r = 0.056 \pm 0.020$
Planck with priors, CPL	$w_0 = -1.1 \pm 0.2$	$w_0 = -1.1 \pm 0.2$
all experiments, CPL	$w_0 = -1.1 \pm 0.2$	$w_0 = -1.1 \pm 0.2$
Planck with priors, CPL	$w_a = 0.3 \pm 0.6$	$w_a = 0.3 \pm 0.6$
all experiments, CPL	$w_a = 0.3 \pm 0.6$	$w_a = 0.2 \pm 0.6$

Table 4. 2σ upper limits and 1σ uncertainties for the measurements of r for the null and positive detection cases, and 1σ uncertainties for the measurements of the CPL parameters w_0, w_a for the different expansion models and dataset combinations.

These limits have been derived from one-dimensional contours, which are shown in Fig. 6, reporting the null detection case only, for simplicity, for r and the DE parameters, and restricting to the case of DE models with $w > -1$; it can be noticed how considering the whole CMB datasets yields an improvement on the detection of r , reflecting Table 4, while almost no difference is noticeable between the cases of dynamical DE or Λ . Looking at the first panel in Fig. 6 one can in particular appreciate how the shape in the likelihood for r is non-Gaussian, justifying our choice of going through a MCMC analysis rather than relying

on a Fisher matrix approach. For DE parameters, we notice no particular improvement in considering the case of all CMB or pure satellite datasets alongside SNe, BAO and HST data. The same holds when looking at two-dimensional contours, shown in Fig. 7 in the (r, w_0) , (r, w_a) and (w_0, w_a) planes, for the null (blue) and positive (red) detection cases: in none of the three panels a significant improvement in DE parameter recovery is shown, even allowing for cosmologies with $w < -1$. We also notice that no degeneracies among these parameters are detectable with the datasets we consider. The figures also quantify the precision achievable on DE parameters, being comparable and of the order of a few ten percents, for both parameters and both fiducial models.

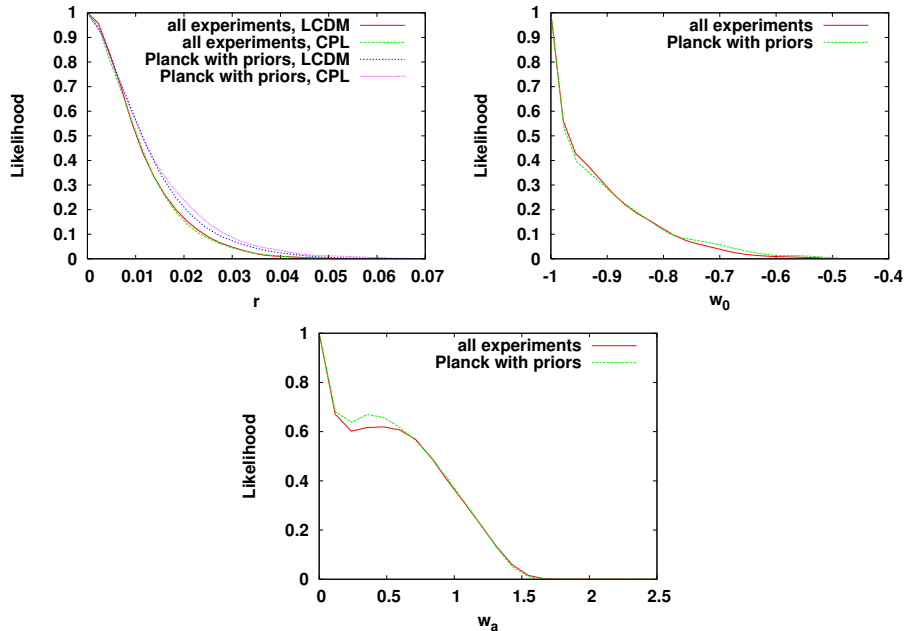


Figure 6. One-dimensional contours for r , w_0 and w_a respectively, in the case of null detection for r ; all plots show differences when using satellite, or all CMB datasets; the plot for r also includes the Λ CDM cases.

Finally, we show other relevant two-dimensional contour plots for the case of null detection (Fig. 8) and for the $r = 0.05$ fiducial value (Fig. 9), highlighting how with the data considered here it is not possible to detect any degeneracy between the primordial tensorial mode parameter r and other cosmological parameters. Despite this remarkable result, we stress that our results concern a nominal performance of the various datasets, and in particular do not consider foreground cleaning or other systematic effects, which were pointed out as possible sources of bias for r in previous works [33, 34, 47].

5 Concluding remarks

The primordial Gravitational Waves (PGWs) and lensing power constitute the dominant effects for the B -mode polarization in the anisotropies of the Cosmic Microwave Background (CMB). While the former is dominated by the physics of the early Universe, parametrized through the primordial tensor-to-scalar ratio r , the latter is instead due to structure formation, and thus influenced by the expansion rate at the epoch of the onset of cosmic acceleration. This, in turn, is dependent on the underlying dynamics of the Dark Energy (DE).

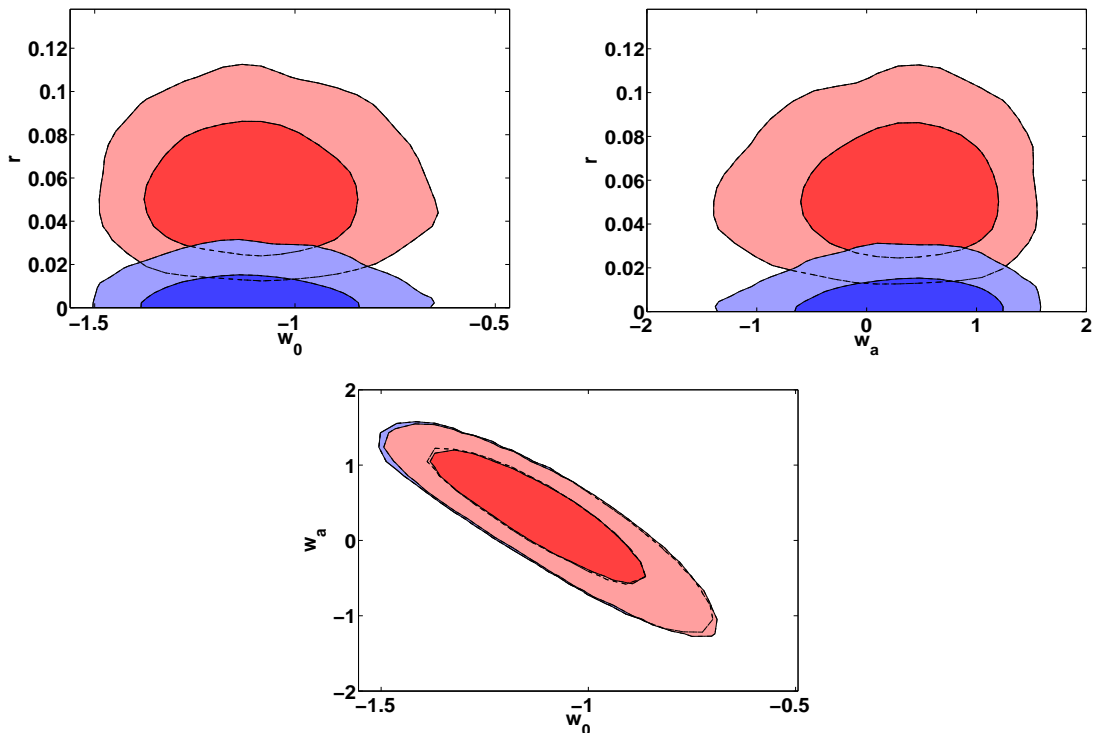


Figure 7. Up, left panel: 1 and 2σ contours $w_0 - r$ diagram for the combination of all considered datasets. In blue, the upper limit on the simulated data with fiducial value $r = 0$. In red, the case of simulated data with fiducial value $r = 0.05$. Up, right panel: 1 and 2σ contours $w_a - r$ diagram. In blue, the upper limit on the simulated data with fiducial value $r = 0$. In red, the case of simulated data with fiducial value $r = 0.05$. Lower panel: 1 and 2σ contours $w_0 - w_a$ diagram. In blue, the constraints on the simulated data with fiducial value $r = 0$. In red, the case of simulated data with fiducial value $r = 0.05$.

Despite both signals being present in the CMB B -modes, their joint measurement in terms of parameter estimation was never considered, and this work represents a first step in this direction.

We first address the lensing relevance for constraining our parametrization of the expansion history, assuming no PGWs. We find comparable results when the lensing is extracted from T and E data and when the lensing is traced directly through lensing B -modes, by forthcoming satellite and sub-orbital data, respectively, both for a Planck experiment and for a CMBpol experiment. Focusing on the latter case, where the two processes directly compete for detection in B -modes, we quantify the constraining power on the abundance of PGWs which is expected from combined forthcoming satellite and sub-orbital experiments probing CMB polarization in cosmologies with generalized expansion histories, parametrized through the present and first redshift derivative of the DE equation of state, w_0 and w_a , respectively. We find that in the case of pure satellite measurements, corresponding to the Planck nominal performance, the constraining power on GWs power is weakened by the inclusion of the extra degrees of freedom, resulting in an increase of about 10% of the upper limits on r in fiducial models with no GWs, as well as a comparable increase in the error bars in models with non-zero tensor power. The inclusion of sub-orbital CMB experiments, capable of mapping the B -mode power up to the angular scales which are affected by lensing, has the effect

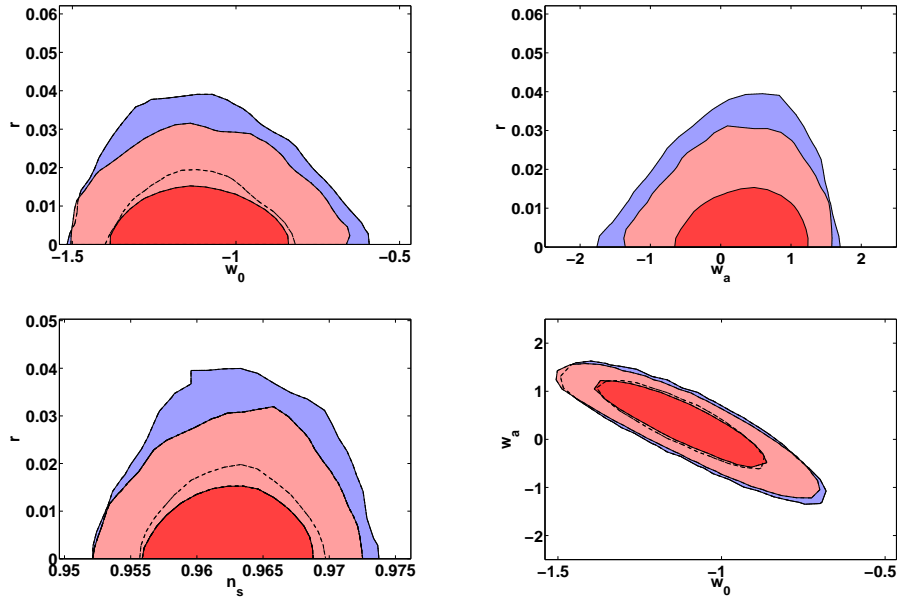


Figure 8. Results from the analysis on the $r = 0$ fiducial value simulated dataset. In all plots, blue contours represent pure satellite CMB data, while the red ones include sub-orbital ones as well. From left to right, from top to bottom. 1. $1 - 2\sigma$ contours for $r - w_0$. 2. $1 - 2\sigma$ contours for $r - w_a$. 3. $1 - 2\sigma$ contours for $r - n_s$ for dynamical DE. 4. $1 - 2\sigma$ contours for $w_0 - w_a$.

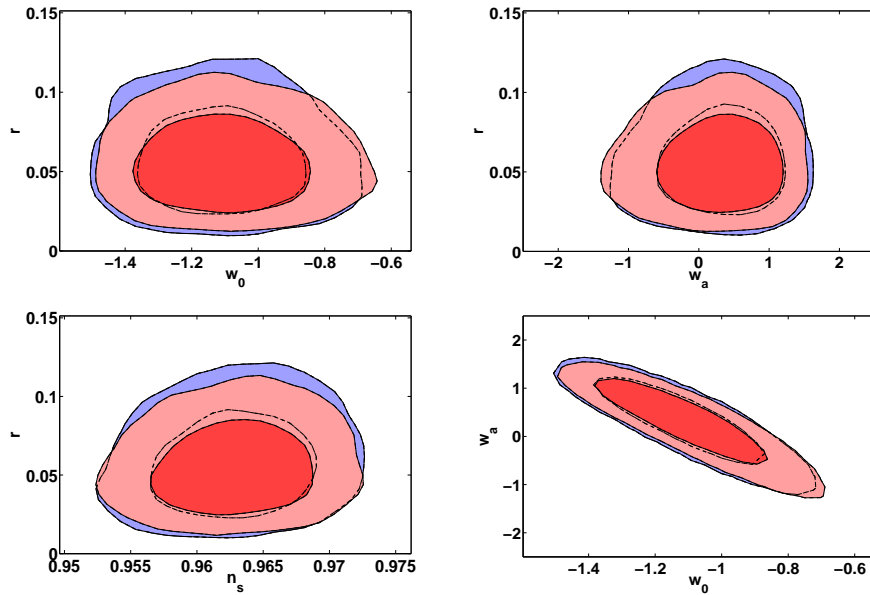


Figure 9. Results from the analysis on the $r = 0.05$ fiducial value simulated dataset. In all plots, blue contours represent pure satellite CMB data, while the red ones include sub-orbital ones as well. From left to right, from top to bottom. 1. $1 - 2\sigma$ contours for $r - w_0$. 2. $1 - 2\sigma$ contours for $r - w_a$. 3. $1 - 2\sigma$ contours for $r - n_s$ for dynamical DE. 4. $1 - 2\sigma$ contours for $w_0 - w_a$.

of making such loss of constraining power vanishing below a detectable level. We interpret these results as a joint effect of the CMB and external datasets: the former are able, in particular with the data from sub-orbital probes, to access the region of B -modes which is lensing dominated, and therefore sensitive to the DE abundance at the onset of acceleration; the latter, as the case of Type Ia SNe and the Hubble Space Telescope, are on the other hand strongly constraining the dynamics of cosmic expansion at present. By inspecting the constraints on all cosmological parameters, including those parametrizing the expansion history, we also show that the datasets we consider do not highlight new degeneracies in the parametrization we consider.

Our results indicate that the combination of satellite and sub-orbital CMB data, with the available external data useful to inquire the late time expansion history, can be used for constraining jointly the dynamics of the DE as well as the primordial tensor-to-scalar ratio, with no new degeneracies or significant loss of sensitivity in particular on r with respect to the case in which a pure Cosmological Constant determines the late time cosmological expansion. Our assumptions of course include the nominal performance of these experiments, and no realistic data analysis consisting in the inclusion of foregrounds in the CMB data, as well as systematic errors. It would be interesting to further investigate this phenomenology in specific DE models, and considering the role of future surveys in giving more accurate constraints.

Acknowledgements

This work was supported by the INFN PD51 initiative. MM wants to thank Erminia Calabrese for useful computational discussions and information. CA thanks Fabio Noviello for his comments and useful discussion. CB also acknowledges support by the Italian Space Agency through the ASI contracts Euclid-IC (I/031/10/0).

References

- [1] Smoot, G. F., Bennett, C. L. et al., Structure in the COBE differential microwave radiometer first-year maps. *Astrophys. J. Lett.* **396**, L1 (1992).
- [2] Komatsu E., et al., Seven-Year Wilkinson Microwave Anisotropy Probe (WMAP) Observations: Cosmological Interpretation. *Astrophys. J. Supp.* **192**, 18 (2011).
- [3] The Planck Collaboration, Planck early results. I. The Planck mission. *Astron. & Astrophys.* **536**, A1 (2011).
- [4] Kamionkowski M., Kosowsky A., Stebbins A., Statistics of cosmic microwave background polarization. *Phys. Rev. D* **55**, 7368 (1997).
- [5] Zaldarriaga M., Seljak U., All-sky analysis of polarization in the microwave background. *Phys. Rev. D* **55**, 1830 (1997).
- [6] Zaldarriaga M., Seljak U., Gravitational lensing effect on cosmic microwave background polarization. *Phys. Rev. D* **58**, 023003 (1998).
- [7] Hlozek R., et al., The Atacama Cosmology Telescope: a measurement of the primordial power spectrum. *Astrophys. J.* **740**, article id. 90 (2012).
- [8] Keisler R., et al., Measurement of the damping tail of the Cosmic Microwave Background Power Spectrum with the South Pole Telescope. *Astrophys. J.* **743**, article id. 28 (2011).
- [9] Sherwin, B. D., Das, S., et al., The Atacama Cosmology Telescope: Cross-Correlation of CMB Lensing and Quasars. eprint arXiv:1207.4543 (2012).
- [10] The Quiet Collaboration, First Season QUIET Observations: Measurements of Cosmic Microwave Background Polarization Power Spectra at 43 GHz in the Multipole Range $25 \leq \ell \leq 475$. *Astrophys. J.* **741**, 111 (2011).
- [11] Zhang, Y., Yuan, Y. Zhao, W., and Chen, Y., Relic Gravitational Waves in the Accelerating Universe. *Classical and Quantum Gravity* **22**, 1383-1394 (2005)
- [12] Hirata C. M., Seljak U., Reconstruction of lensing from the cosmic microwave background polarization. *Phys. Rev. D* **69**, 043005 (2004).
- [13] Acquaviva V., Baccigalupi C., Dark Energy records in lensed cosmic microwave background. *Phys. Rev. D* **74**, 103510 (2006).
- [14] Hu W., Huterer D., Smith K.M., Supernovae, the Lensed Cosmic Microwave Background, and Dark Energy. *Astrophys. J. Lett.* **650**, L13 (2006).
- [15] Sherwin B.D., et al., Evidence for Dark Energy from the Cosmic Microwave Background Alone Using the Atacama Cosmology Telescope Lensing Measurements. *Phys. Rev. Lett.* **107**, 021302 (2011).
- [16] Reichborn-Kjennerud B., et al., EBEX: A balloon-borne CMB polarization experiment. Millimeter, Submillimeter, and Far-Infrared Detectors and Instrumentation for Astronomy V. Edited by Holland, Wayne S.; Zmuidzinas, Jonas. Proceedings of the SPIE, **7741**, 77411C (2010).

- [17] Keating, B., Moyerman, S. et al. Ultra High Energy Cosmology with POLARBEAR arXiv:1110.2101 (2011).
- [18] Planck collaboration, The Scientific Programme of Planck. arXiv:astro-ph/0604069v1 (2006).
- [19] Chevallier M., Polarski D., Accelerating Universes with Scaling Dark Matter. International Journal of Modern Physics D **10** (2001).
- [20] Linder E. V., Mapping the Dark Energy Equation of State. Maps of the Cosmos, ASP conference series, IAU Symposium **216** (2003).
- [21] Hu, W., Weak Lensing of the CMB: A Harmonic Approach. *Phys. Rev. D* **62**, 4 (2000).
- [22] Bartelmann M., Schneider P., Weak Gravitational Lensing, *Phys. Rept.* **340**, 291 (2001).
- [23] Hanson D., Challinor A., Lewis A., Weak lensing of the CMB. *General Relativity and Gravitation*, **42**, 9 (2010).
- [24] Perotto L., Lesgourgues J., Hannestad S., Tu H., Wong Y. Y. Y., Probing cosmological parameters with the CMB: Forecasts from full Monte Carlo simulations, *JCAP* **0610** (2006) 013.
- [25] Calabrese E. et al., CMB Lensing Constraints on Dark Energy and Modified Gravity Scenarios, *Phys. Rev. D* **80** (2009) 103516.
- [26] Okamoto T., Hu W., CMB Lensing Reconstruction on the Full Sky, *Phys. Rev. D* **67** (2003).
- [27] Seljak, U., Hirata, C. M., Gravitational lensing as a contaminant of the gravity wave signal in the CMB. *Phys. Rev. D* **69**, 4 (2004).
- [28] Efstathiou G., Principal component analysis of the cosmic microwave background anisotropies: revealing the tensor degeneracy, *Mon. Not. Roy. Astron. Soc.* **332** 193 (2002).
- [29] Di Valentino E., Melchiorri A., Pagano L., Testing the Inflationary Null Energy Condition with Current and Future Cosmic Microwave Background Data, *Int. J. Mod. Phys. D* **20**, 1183 (2011).
- [30] Wolz L., Kilbinger M., Weller J., Giannantonio T., On the Validity of Cosmological Fisher Matrix Forecasts, *J. Cosm. Astroparticle Phys.* Issue 09 (2012)
- [31] Lewis, A., Bridle, S., Cosmological parameters from CMB and other data: A Monte Carlo approach. *Phys. Rev. D* **66**, 103511 (2002).
- [32] Miller, N.J., Shimon, M., Keating, B.G., CMB Beam Systematics: Impact on Lensing Parameter Estimation. *Phys. Rev. D* **79**, 6 (2009).
- [33] Fantaye Y., et al., Estimating the tensor-to-scalar ratio and the effect of residual foreground contamination. *J. Cosm. Astroparticle Phys.* **8**, 1 (2011).
- [34] Stivoli F., et al., Maximum likelihood, parametric component separation and CMB B-mode detection in suborbital experiments. *MNRAS* **408**, 2319 (2010).
- [35] Gelman, A., Rubin, D.B., Inference from iterative simulation using multiple sequences, *Statistical Science*, **7**, 457-511 (1992).
- [36] Blake, C., et al., Blake, C., Kazin E., et al., The WiggleZ Dark Energy Survey: mapping the distance-redshift relation with baryon acoustic oscillations. *MNRAS* **418**, 1707 (2011).
- [37] Percival W.J., et al., Baryon Acoustic Oscillations in the Sloan Digital Sky Survey Data Release 7 Galaxy Sample. *MNRAS* **417**, 3101 (2009).
- [38] Kessler R., et al., First-year Sloan Digital Sky Survey-II (SDSS-II) Supernova Results: Hubble Diagram and Cosmological Parameters. *Astrophys. J. Supp.* **185**, 32 (2009).
- [39] Riess A.G., et al., A Redetermination of the Hubble Constant with the Hubble Space Telescope from a Differential Distance Ladder. *Astrophys. J.* **699**, 539 (2009).

- [40] Bock, J., Aljabri, A., et al., Study of the Experimental Probe of Inflationary Cosmology (EPIC)-Intermediate Mission for NASA's Einstein Inflation Probe. arXiv:0906.1188 (2009).
- [41] Armitage-Caplan, C., et al. for the CORE collaboration, CORE (Cosmic Origins Explorer) A White Paper, arXiv:1102.2181 (2011).
- [42] Van Engelen, A., Keisler, R., et al., A Measurement of Gravitational Lensing of the Microwave Background Using South Pole Telescope Data. *Astrophys. J.* **756** (2012).
- [43] Perotto, L., Bobin, J., Plaszczynski, et al., Reconstruction of the CMB lensing for Planck, *Astron. & Astrophys.* **519** (2010).
- [44] Fantaye, Y., Baccigalupi, C., Leach, S., Yadav, A. P. S., CMB lensing reconstruction in the presence of diffuse polarized foregrounds. arXiv:1207.0508 (2012).
- [45] Stephen P. Brooks, Andrew Gelman, *General Methods for Monitoring Convergence of Iterative Simulations* Journal of Computational and Graphical Statistics, Vol. 7, Iss. 4, 1998
- [46] Efstathiou G., Gratton S., B-mode Detection with an Extended Planck Mission, JCAP **0906** 011 (2009).
- [47] Pagano L., et al., CMB polarization systematics, cosmological birefringence, and the gravitational waves background. *Phys. Rev. D* **80**, 043522 (2009).